

# Sloshing Suppression Control by using Physical Boundary Element Model and Predictive Control in Liquid Container Transfer System

Hisashi Okatsuka<sup>1</sup>, Ryota Shibuya<sup>1</sup>, Kazuhiko Terashima<sup>1</sup>, Yoshiyuki Noda<sup>2</sup> and Yoshiki Matsuo<sup>3</sup>

<sup>1</sup>*Department of Mechanical Engineering, Toyohashi University of Technology,  
Hibarigaoka 1-1, Tempaku, Toyohashi, Aichi 441-8580, Japan*

<sup>2</sup>*Department of Mechanical System Engineering, Faculty of Engineering, University of Yamanashi,  
Takeda 4-4-37, Kofu, Yamanashi 440-0016, Japan*

<sup>3</sup>*Department of Computer Science, Tokyo University of Technology,  
1404-1 Katakuramachi, Hachioji City, Tokyo 192-0982, Japan*

**Keywords:** Sloshing Control, Boundary Element Method, Generalized Predictive Control.

**Abstract:** This paper presents sloshing suppression control of liquid transferred at a desirable-speed. In order to suppress sloshing, a mathematical model consisting of continuous equations and the pressure equation is used and the sloshing phenomena are analyzed by using the Boundary Element Method (BEM). Further, the BEM model is transformed into the state-variable model. The proposed model can estimate not only first-order mode sloshing but also higher-order mode sloshing and predict the future behavior of liquid level more precisely. Moreover, sloshing is suppressed by using Model Predictive Control (MPC). We were able to transfer the container while minimizing sloshing and maintaining a desirable speed.

## 1 INTRODUCTION

In recent years, multi-kind and small-quantity production has become mainstream in manufacturing industry to meet customer needs. However, increasing complexity of manufacturing lines and the rising number of processes have resulted in higher manufacturing costs and the need for frequent maintenance. Furthermore, types of liquid products range from food to chemicals and molten metals. Piping systems are generally used for transferring these liquid products. High-pressure water techniques using pumps are widely applied for washing these piping systems. However, the need for frequent washing and maintenance has led to cost increases and deterioration of production efficiency. Therefore, there is a need for a reasonable liquid transfer system with ease of maintenance and a simple mechanism.

In this paper, we propose a transfer system for liquid containers, which is combined with a servo motor. The proposed system is easy to maintain. However, during high-speed transfer of containers, sloshing (liquid vibration) occurs on the liquid surface and may cause liquid overflow and/or quality deterioration owing to entrainment of air or gases. Therefore, a new approach is required to enable transferring

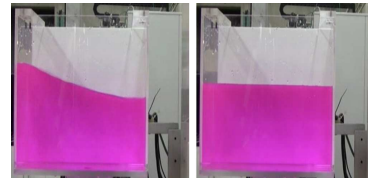


Figure 1: Photos of experimental results.

liquid containers at a desirable speed while suppressing sloshing.

Fig. 1 shows the motion of the liquid surface. The left photo shows the case without control and the right photo shows the case with control. These are images captured when the container was stopped after being transferred for 0.3 m.

Concerning sloshing analysis, computer simulation and anti-slosh structure design, much research has been reported since the 1960s (Abramson and Chu, 1966) (Ibrahim, 2005). On the other hand, dynamic control of sloshing has been studied since 1990. Major studies on sloshing control include one using a simple pendulum and an optimal servo system combined with a kalman filter (Hamaguchi et al., 1994). Yano, Oguro and Terashima (Yano et al., 2001) omitted the frequency area of the input signal around the peak of the transfer function in or-

der to eliminate vibration. Furthermore, Romero et al. referred to many reports concerning numerical analysis of liquid in rectangular containers subjected to horizontal acceleration (Romero and Ingber, 1995). Feddema et al. (Feddema et al., 1997) proposed methods for controlling the surface of a liquid in an open container by altering the horizontal acceleration or by tilting the container parallel with the liquid surface in order to suppress sloshing. Mathematical models that have been proposed are mostly for the first-order mode sloshing in order to suppress vibration on the walls of containers. However, in a container transferred at a reasonable speed, higher-order model of vibration is caused, and it is impossible to estimate sloshing accurately by using the conventional model.

Other research applies the Boundary Element Method (BEM) (Nakayama and Washizu, 1981) to divide the liquid surface into multiple boundary points and calculate the surface displacement at each point. For this analysis, the continuous formula of the liquid and the boundary condition of the surface are necessary. When this approach is applied to sloshing control, the modal model with a suitable degree is built, where model parameters are identified by the curve fitting method, comparing with the results of BEM simulations (Hamaguchi et al., 1995). This procedure causes the mathematical model based on BEM to lose its physical structure and be transformed into a black-box model. Therefore, in this paper, a BEM model (Okatsuka et al., 2002) is translated to a state space model based on physical differential equations expressing the liquid surface displacement.

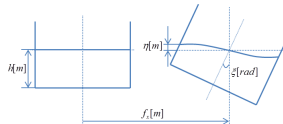


Figure 2: Analytical model of liquid container.

This linear system clarifies the relations between inputs and outputs, including the higher-mode vibration, and enables reasonable control of sloshing, when combined with modern control theory. The optimum control of sloshing is achieved by the combination with model predictive control (MPC). With regard to MPC, generalized predictive control (GPC) (Oshima, 2000) (Masuda et al., 2000) is used in this paper.

## 2 BASIC EQUATIONS AND ANALYSIS CONDITIONS

In this section, we explain the governing equations (Kimura et al., 1996), analysis conditions and the

target container.

- $\Omega$  is the area occupied with liquid. The boundary  $\Gamma$  is composed of two boundaries,  $\Gamma_f$  and  $\Gamma_w$ .  $\Gamma_f$  is the free surface in contact with the air and  $\Gamma_w$  is the wall surface. Thus,  $\Gamma = \Gamma_f + \Gamma_w$ .
- The number of elements by BEM: Total of 60 elements comprising 20 elements on the free surface and on the bottom, respectively, and 10 elements on the side wall. Elements are counted counter-clockwise at the boundary.
- The liquid is a perfect fluid that has no vortex or viscosity, and is incompressible. The pressure on the free surface is constant, and the displacement is assumed to be minute.
- The center of moving and pitching vibration  $C(x_c, 0, z_c)$  is on the z-axis ( $x_c = 0$ ).
- The velocity potential  $\Phi(x, z, t)$  is defined by the relative velocity of the liquid corresponding to the container.
- The control value (output), the displacement from the liquid surface at rest  $\eta(x, t)$  [m], is the motion relative to the container.
- The manipulator forces are the displacement acceleration  $\ddot{f}_X(t)$  [m/s<sup>2</sup>] in the X direction and the angular acceleration of pitching excitation  $\ddot{\xi}(t)$  [rad/s<sup>2</sup>]. These forces are moved by a manipulator through the control signal. The forced displacement in the Z-direction  $f_z(t)$  [m] = 0.

$$\frac{\partial^2 \Phi}{\partial x^2} + \frac{\partial^2 \Phi}{\partial z^2} = 0 \quad (1)$$

$$\left. \frac{\partial \Phi}{\partial x} \right|_{x=\pm a} = 0 \quad \left. \frac{\partial \Phi}{\partial z} \right|_{z=0} = 0 \quad ; \text{ on } \Gamma_w \quad (2)$$

$$\left. \frac{\partial \Phi}{\partial t} \right|_{z=h+\eta} + x[\ddot{f}_X - g * \xi] + x[(h - z_c)\ddot{\xi}] + g * (\eta + h + f_z) = 0 \quad (3)$$

$$\left. \frac{\partial \Phi}{\partial t} \right|_{z=h+\eta} = \frac{\partial \eta}{\partial t} - 2x\dot{\xi} \quad ; \text{ on } \Gamma_f \quad (4)$$

- (1). Laplace equation; expressing the condition of continuity inside the liquid
- (2). Adaptable condition on the side wall and the base
- (3). Dynamic boundary condition on the liquid surface
- (4). Kinematic boundary condition on the liquid surface

In the above-mentioned basic equations, non-linear parts are eliminated. Hereafter,  $f_z = 0$  in all equations.

### 3 DERIVATION OF THE BOUNDARY INTEGRAL EQUATION

Assuming  $\zeta$  and  $x(x, z)$  as the random point on the boundary, the boundary problem of two dimensions is solved using the weighted residual expression. Here,  $\alpha$  is the internal angle at the point  $\zeta$ .

$$\frac{\alpha(\zeta)}{2\pi} \Phi(\zeta, t) + \int_{\Gamma} \Phi(\mathbf{x}, t) q^*(\mathbf{x}, \zeta) d\Gamma(\mathbf{x}) - \int_{\Gamma} \frac{\partial \Phi}{\partial n} v^*(\mathbf{x}, \zeta) d\Gamma(\mathbf{x}) = 0 \quad (5)$$

Here, the following formulas are employed as the basic solutions. Here,  $B!H(BnB!l(B$  shows the outward normal at the boundary.

$$q^*(\mathbf{x}, \zeta) = \frac{1}{2\pi} \frac{\partial}{\partial n} \left( \ln \frac{1}{r} \right), \quad v^*(\mathbf{x}, \zeta) = \frac{1}{2\pi} \left( \ln \frac{1}{r} \right),$$

where  $r = \|\mathbf{x} - \zeta\|$ . Substitute the boundary conditions Eq. 2 and Eq. 4 into the Eq. 5, where  $\partial \Phi / \partial n = \partial \Phi / \partial z$ , and the following equation is obtained:

$$\frac{\alpha(\zeta)}{2\pi} \Phi(\zeta, t) + \int_{\Gamma_f + \Gamma_w} \Phi(\mathbf{x}, t) q^*(\mathbf{x}, \zeta) d\Gamma(\mathbf{x}) - \int_{\Gamma_f} [\dot{\eta}(\mathbf{x}, t) - 2x\dot{\xi}] v^*(\mathbf{x}, \zeta) d\Gamma(\mathbf{x}) = 0$$

In order to solve the above equation using the boundary collocation method<sup>1</sup>, suppose  $\mathbf{x}_i (i = 1, 2, \dots, N)$  as the coordinates of the collocation. Then, the following equation is obtained:

$$\frac{\alpha(\mathbf{x}_i)}{2\pi} \Phi(\mathbf{x}_i, t) + \int_{\Gamma_f + \Gamma_w} \Phi(\mathbf{x}, t) q^*(\mathbf{x}, \mathbf{x}_i) d\Gamma(\mathbf{x}) - \int_{\Gamma_f} [\dot{\eta}(\mathbf{x}, t) - 2x\dot{\xi}] v^*(\mathbf{x}, \mathbf{x}_i) d\Gamma(\mathbf{x}) = 0 \quad (6)$$

Concerning Eq. 3, which represents the dynamical boundary condition, we suppose that the first  $M$  pieces  $\mathbf{x}_j (j = 1, 2, \dots, M)$  of collocation (in all pieces) exist on the free surface  $\Gamma_f$ .

$$\dot{\Phi}(\mathbf{x}_j, t) + x_j [\ddot{f}_X - g * \xi] + x_j [(h - z_c) \ddot{\xi}] + g(\eta(\mathbf{x}_j, t) + h) = 0 \quad (7)$$

By these procedures, the basic equations (Eq.1 ~ Eq.4) are transformed to simultaneous equations comprising an integral equation (6) and a boundary condition (7).

<sup>1</sup>The Boundary collocation method selects limited points on the boundary and makes the residual zero.

### 4 DISCRETE-TIME SYSTEM AND STATE EQUATIONS

In order to organize a discrete-time system, the boundary  $\Gamma$  is divided into many straight-line elements, and Eq. 6 becomes as follows. However, the values of  $\Phi$  and  $\eta$  in each element are fixed.

$$\frac{\alpha(\mathbf{x}_i)}{2\pi} \Phi(\mathbf{x}_i, t) + \sum_{\Gamma_f + \Gamma_w} \left( \int_{e_j} \Phi(\mathbf{x}, t) q^*(\mathbf{x}, \mathbf{x}_i) d\Gamma(\mathbf{x}) \right) - \sum_{\Gamma_f} \left( \int_{e_j} [\dot{\eta}(\mathbf{x}, t) - 2x\dot{\xi}] v^*(\mathbf{x}, \mathbf{x}_i) d\Gamma(\mathbf{x}) \right) = 0 \quad (8)$$

where  $\Phi(\mathbf{x}, t) = \Phi(\mathbf{x}_j, t) = \Phi_j$ ,  $\dot{\eta}(\mathbf{x}, t) = \dot{\eta}(\mathbf{x}_j, t) = \dot{\eta}_j$  and  $\alpha(\mathbf{x}_i) = \pi$

$$\frac{1}{2} \Phi(\mathbf{x}_i, t) + \sum_{\Gamma_f + \Gamma_w} \left( \int_{e_j} q^*(\mathbf{x}, \mathbf{x}_i) d\Gamma(\mathbf{x}) \right) \Phi_j - \sum_{\Gamma_f} \left( \int_{e_j} v^*(\mathbf{x}, \mathbf{x}_i) d\Gamma(\mathbf{x}) \right) \dot{\eta}_j + 2 \sum_{\Gamma_f} \left( \int_{e_j} v^*(\mathbf{x}, \mathbf{x}_i) d\Gamma(\mathbf{x}) \right) x_j \dot{\xi} = 0 \quad (9)$$

Furthermore, using the influence parameters  $\hat{H}_{ij}$  and  $G_{ij}$ , defined by the following formulas, Eq. 9 becomes Eq. 10.

$$\hat{H}_{ij} \equiv \int_{e_j} q^*(\mathbf{x}, \mathbf{x}_i) d\Gamma(\mathbf{x}) = \frac{1}{2\pi} \int_{e_j} \frac{\partial}{\partial n(\mathbf{x})} \left( \ln \frac{1}{\|\mathbf{x} - \mathbf{x}_i\|} \right) d\Gamma(\mathbf{x}) \quad (i = 1 \sim 60, j = 1 \sim 60)$$

$$G_{ij} \equiv \int_{e_j} v^*(\mathbf{x}, \mathbf{x}_i) d\Gamma(\mathbf{x}) = \frac{1}{2\pi} \int_{e_j} \left( \ln \frac{1}{\|\mathbf{x} - \mathbf{x}_i\|} \right) d\Gamma(\mathbf{x}) \quad (i = 1 \sim 60, j = 1 \sim 20)$$

$$\frac{1}{2} \Phi(\mathbf{x}_i, t) + \sum_{\Gamma_f + \Gamma_w} \hat{H}_{ij} \Phi_j = \sum_{\Gamma_f} G_{ij} \dot{\eta}_j - 2 \sum_{\Gamma_f} G_{ij} x_j \dot{\xi} \quad (10)$$

Next, in order to arrange the left side for  $\Phi_j$ , substitute  $\hat{H}_{ij}$  by  $H_{ij}$  (here,  $\hat{H}_{ij} = 0$  for  $i=j$ ),<sup>2</sup> and the following is obtained:

$$H_{ij} \equiv \frac{1}{2} \delta_{ij} + \hat{H}_{ij} = \hat{H}_{ij} \quad (i \neq j) (\delta_{ij} = 0)$$

$$H_{ij} \equiv \frac{1}{2} \delta_{ij} + \hat{H}_{ij} = \frac{1}{2} \quad (i = j) (\delta_{ij} = 1)$$

<sup>2</sup>When the collocation is consistent with the node, the normal vector at point X intersect orthogonally with the vector  $(X - X_i)$

The output equation is as follows :

$$\sum_{j=1}^M G_{ij} \dot{\eta}_j = \sum_{j=1}^N H_{ij} \Phi_j + 2 \sum_{j=1}^M G_{ij} x_j \ddot{\xi} \quad (N > M, i = 1, 2, \dots, N) \quad (11)$$

Furthermore, divide Eq. 11, top and bottom, right and left, in order to eliminate  $\Phi$  that is larger than  $M$ .

$$\begin{pmatrix} \eta_1 \\ \vdots \\ \eta_M \end{pmatrix} = (P^{-1}Q) \begin{pmatrix} \Phi_1 \\ \vdots \\ \Phi_M \end{pmatrix} + 2 \begin{pmatrix} x_1 \\ \vdots \\ x_M \end{pmatrix} \ddot{\xi}, \quad (12)$$

where

$$\begin{aligned} P &= (\mathbf{G}_1) - (\mathbf{H}_2)(\mathbf{H}_4)^{-1}(\mathbf{G}_2) \\ Q &= (\mathbf{H}_1) - (\mathbf{H}_2)(\mathbf{H}_4)^{-1}(\mathbf{H}_3) \\ \mathbf{G}_1 &= G_{ij} (1 \leq i \leq M, 1 \leq j \leq M) \\ \mathbf{H}_1 &= H_{ij} (1 \leq i \leq M, 1 \leq j \leq M) \end{aligned} \quad (13)$$

$\mathbf{H}_2, \mathbf{G}_2, \mathbf{H}_3, \mathbf{H}_4$  are similar to above. Next, in the dynamic boundary Eq. 7 for the free liquid surface, leave the differential item on the left side of the equal sign:

$$\begin{pmatrix} \Phi_1 \\ \vdots \\ \Phi_M \end{pmatrix} = -g \begin{pmatrix} \eta_1 \\ \vdots \\ \eta_M \end{pmatrix} + [(z_c - h)x_j \ddot{\xi}] + gx_j \ddot{\xi} - (\ddot{f}_X x_j + gh) \quad (j = 1, 2, \dots, M) \quad (14)$$

Exciting angular acceleration and exciting angular velocity are as follows :

$$\begin{pmatrix} \dot{\xi} \\ \ddot{\xi} \end{pmatrix} = \begin{pmatrix} \xi \\ \dot{\xi} \end{pmatrix}$$

Consequently, the state equation using a state variable vector of  $\mathbf{X} = (\Phi_1 \dots \Phi_M, \eta_1 \dots \eta_M, \xi, \dot{\xi})^T$  becomes

$$\dot{\mathbf{X}} = \mathbf{A}\mathbf{X} + \mathbf{b} \begin{pmatrix} \ddot{\xi} \\ \dot{f}_X \\ h \end{pmatrix}, \quad (15)$$

where

$$\mathbf{A} = \begin{pmatrix} 0_M & -gI_M & 0 & gx_j \\ (P^{-1}Q) & 0_M & 2x_j & 0 \\ 0 & 0 & 0 & 0 \\ 0 & 0 & 1 & 0 \end{pmatrix},$$

$$\mathbf{b} = \begin{pmatrix} \left. \begin{matrix} -g \\ (z_c - h)x_j & -x_j \\ \vdots \end{matrix} \right\} M \\ \left. \begin{matrix} -g \\ 0 & 0 & 0 \\ \vdots \\ 0 & 0 & 0 \end{matrix} \right\} M \\ \left. \begin{matrix} 1 & 0 & 0 \\ 0 & 0 & 0 \end{matrix} \right\} \end{pmatrix}$$

The output equation is as follows :

$$\mathbf{z} = (\eta_1, \eta_2, \dots, \eta_M) = \mathbf{c}\mathbf{X}, \quad (16)$$

where

$$\mathbf{c} = (0_{1 \dots M}, 1_{1 \dots M}, 0, 0)$$

Furthermore, using MATLAB,  $[\mathbf{A}_G, \mathbf{b}_G] = c2d(\mathbf{A}, \mathbf{b}, \tau)$ , consider  $k$  as the parameter for the sampling period  $\tau (=0.01[s])$ , and the following equation is obtained :

$$\dot{\mathbf{X}}[k+1] = \mathbf{A}_G \mathbf{X}[k] + \mathbf{b}_G \begin{pmatrix} \ddot{\xi}[k] \\ \dot{f}_X[k] \\ h \end{pmatrix} \quad (17)$$

The right side of the Eq. 17,  $\ddot{\xi}[k]$  and  $\dot{f}_X[k]$ , is the control input.

## 5 EXPERIMENTAL APPARATUS AND VERIFICATION OF THE MODEL

The external appearance of the experimental apparatus is shown in Fig. 3. The container made of acrylic resin, which is attached to the end point of the arm supported by the z-axis, is moved by the AC serve motor along the Y-axis (0.3[m] in distance), while rotating around the T-axis. The slender bar vertically mounted on the right side of the container is a level sensor for measuring the behavior of the liquid surface. This sensor is composed of two pieces of stainless wire with a diameter of  $3 \times 10^{-3}[m]$  placed in parallel with an interval of 0.01[m], which are electrodes. Using this apparatus, the values of the simulation and the experimental data are compared.

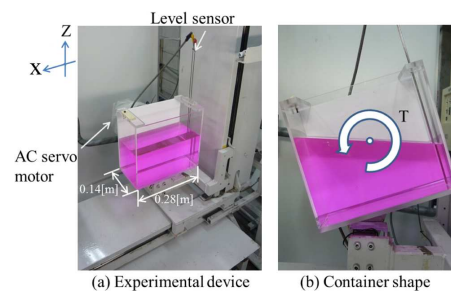


Figure 3: Experimental equipment.

Fig. 4(a), (b) and (c) show transferring position, velocity and acceleration, respectively. Fig. 4(d) shows the estimate and the experimental data for the liquid surface vibration. They are in good agreement.

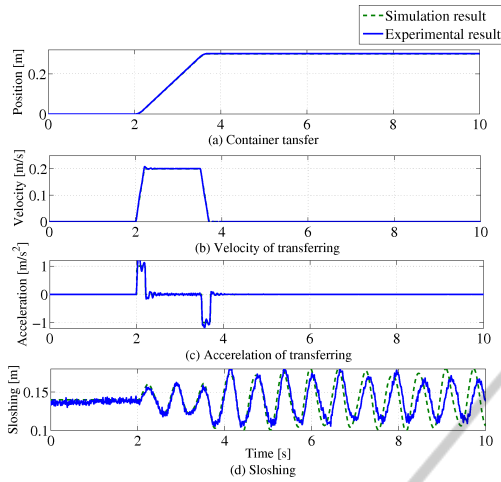


Figure 4: Experimental results for transferring a container.

## 6 DERIVATION OF THE OPTIMAL CONTROL INPUT AND EXPERIMENTAL RESULTS

The state variables  $X$  obtained in the previous section and Eq. 16 and Eq. 17 are shown again. We are able to develop the optimal control law from these items, which constitute a plant model. Since the target value is not step-formed, a special formula including an integrator is not employed. Moreover, instead of the increment of the input, the input itself is used.

$$\mathbf{X} = (\Phi_{1\dots M}, \eta_{1\dots M}, \xi, \xi)^T$$

$$\mathbf{X}[k+1] = \mathbf{A}_G \mathbf{X}[k] + \mathbf{b}_G \begin{pmatrix} \xi[k] \\ \dot{\xi}[k] \\ h \end{pmatrix}$$

$$\mathbf{z}[k] = \mathbf{c} \mathbf{X}[k]$$

Assuming that the value of the angular acceleration  $\ddot{\xi}$  of the container is zero, the above formulas are used again to eliminate the constant terms, and a predictive formula for the output is obtained as follows. Here,  $\mathbf{b}_G = [\mathbf{b}_{G1}, \mathbf{b}_{G2}, \mathbf{b}_{G3}]$

$$\hat{\mathbf{z}}[k+j] = \mathbf{c} \mathbf{A}_G^j \mathbf{X}[k] + \sum_{i=0}^{j-1} \mathbf{c} \mathbf{A}_G^{j-i-1} (\mathbf{b}_{G2} \dot{\xi}[k+i]) \quad (18)$$

The first term of the right side depends on the state at time  $[k]$  and the second term depends on the future control input (on condition that  $0 \leq i \leq j-1$ ). Next, in order to use GPC theory, the following linear quadratic evaluation function is given.  $\mathbf{Q}$  and  $\mathbf{R}$  are the weighted matrix for the liquid surface variation

and control input.

$$J = \sum_{j=N_1}^{N_2} \hat{\mathbf{z}}[k+j]^T \mathbf{Q} \hat{\mathbf{z}}[k+j] + \sum_{j=1}^{N_u} \ddot{f}_X[k+j-1]^T \mathbf{R} \ddot{f}_X[k+j-1] \quad (19)$$

The above formula is obtained from two conditions. Firstly, the future target for the output is zero. Secondly,  $\ddot{f}_X$  is applied for the input.  $N_1$  and  $N_2$  are the minimum and maximum prediction area, respectively, and  $N_u$  is the control prediction area. We adopted  $N_1 = 1, N_2 = 4$  and  $N_u = 3$ . We used as small values as possible for  $N_1, N_2$  and  $N_u$  in order to increase the calculation speed of the experimental apparatus. As the results obtained by using these values were desirable, we employed these values. Furthermore, concerning  $\mathbf{Q}$  and  $\mathbf{R}$ , considers to become on the same level of size. The predictive formula for output is expressed in the vector form as follows in order to obtain the optimum control law.

$$\mathbf{J} = (\mathbf{Z}[k])^T \mathbf{Q} (\mathbf{Z}[k]) + \mathbf{D}[k]^T \mathbf{R} \mathbf{D}[k], \quad (20)$$

where

$$\mathbf{Z}[k]^T = [\hat{\mathbf{z}}[k+N_1]^T, \dots, \hat{\mathbf{z}}[k+N_2]^T]$$

$$\mathbf{D}[k]^T = [\ddot{f}_X[k]^T, \dots, \ddot{f}_X[k+N_u-1]^T]$$

$$\mathbf{Z}[k] = \mathbf{G}_s \mathbf{D}[k] + \mathbf{H}_s \mathbf{X}[k] \quad (21)$$

$$\mathbf{G}_s = \begin{pmatrix} \mathbf{c} \mathbf{b}_{G1} & 0 & 0 \\ \mathbf{c} \mathbf{A}_G \mathbf{b}_{G1} & \mathbf{c} \mathbf{b}_{G1} & 0 \\ \mathbf{c} \mathbf{A}_G^2 \mathbf{b}_{G1} & \mathbf{c} \mathbf{A}_G \mathbf{b}_{G1} & \mathbf{c} \mathbf{b}_{G1} \\ \mathbf{c} \mathbf{A}_G^3 \mathbf{b}_{G1} & \mathbf{c} \mathbf{A}_G^2 \mathbf{b}_{G1} & \mathbf{c} \mathbf{A}_G \mathbf{b}_{G1} \end{pmatrix},$$

$$\mathbf{H}_s = (\mathbf{c} \mathbf{A}_G, \mathbf{c} \mathbf{A}_G^2, \mathbf{c} \mathbf{A}_G^3, \mathbf{c} \mathbf{A}_G^4)^T$$

Substitute Eq. 21 into Eq. 20, and the control input  $\mathbf{D}[k]$  that minimizes the value of the evaluation function becomes as follows :

$$\mathbf{D}[k] = (\mathbf{G}_s^T \mathbf{Q} \mathbf{G}_s + \mathbf{R})^{-1} \mathbf{G}_s^T \mathbf{Q} (-\mathbf{H}_s \mathbf{x}[k]) \quad (22)$$

The above control law is effective between time  $[k]$  and time  $[k+N_u-1]$ . However, as mentioned above, the influence of the state of the control object and the disturbance at the current time only are taken into consideration. Therefore, the control law gives the input at the current time only. Thus, the first block of  $\mathbf{D}[k]$  is applied to the control object as follows:-

$$\ddot{f}_X[k] = [\mathbf{I}_m, 0, \dots, 0] \mathbf{D}[k] \quad (23)$$

Fig. 5 shows the control result using GPC. This figure shows good slushing suppression. In order to evaluate the effectiveness of the proposed control method, the proposed method and a conventional method using a notch filter are compared. The notch filter eliminates the input gain based on the slushing natural frequency (Yano and Terashima, 2001). Fig. 6 shows the experimental results.



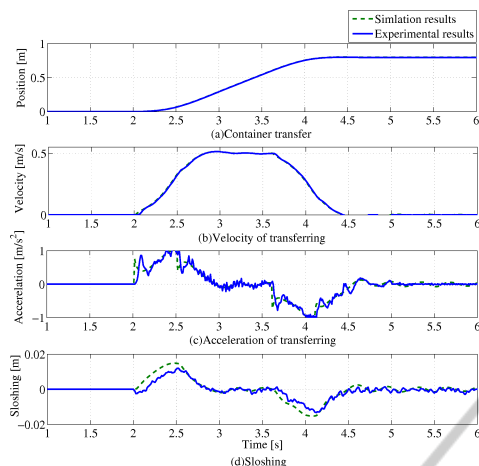


Figure 5: Experimental results (GPC control case).

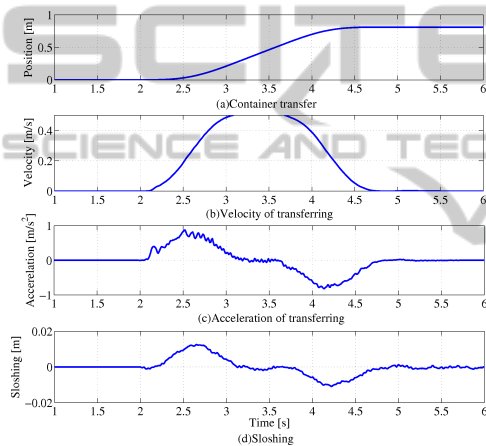


Figure 6: Experimental results (use of a notch filter).

## 7 CONCLUSIONS

Using the state-space equation obtained using BEM, we were able to precisely express the liquid surface vibration during transfer and tilting of a container. Moreover, using GPC, we were able to keep the liquid surface flat during transfer of the container at a constant speed when acceleration is applied in the horizontal direction. In particular, we achieved immediate suppression of sloshing when the container stops. Experimental results provide evidence that our control approach using both the BEM model and MPC achieves better results than any conventional control methods such as the notch filter technique and PID control. Furthermore, useful research based on this paper was reported (Shibuya et al., 2011)

## REFERENCES

- Abramson, H. and Chu, W.H. and Kana, D. (1966). Some studies of non-linear lateral sloshing in rigid containers. *J. Appl. Mechanics, Trans. ASME*, 1966, pages 777–784.
- Feddema, J., Dohrmann, C., Parker, G., Robinett, R., Romero, V., and Schmitt, D. (1997). Control for slosh-free motion of an open container. *IEEE Trans. on Control Systems Technology*, 5(1):29–36.
- Hamaguchi, M., Motegi, H., Terashima, K., and Nomura, N. (1995). Optimal control of transferring a liquid container with boundary element analysis, (in japanese). *Trans. of the Society of Instrument and Control Engineers (SICE)*, 31(9):1442–1451.
- Hamaguchi, M., Terashima, K., and Nomura, H. (1994). Optimal control of transferring a liquid container for several performance specifications, (in japanese). *Trans. of the Japan Society of Mechanical Engineers (JSME) C*, 60(573):1668–1675.
- Ibrahim, R. (2005). *Liquid Sloshing Dynamics*. Cambridge Univ.
- Kimura, K., Takahara, H., and Sakata, M. (1996). Sloshing in a circular cylindrical tank subjected to pitching excitation (condition for liquid surface remaining plane). *Trans. of the Japan Society of Mechanical Engineers (JSME)*, (96-1):1321.
- Masuda, S., Shah, S., and Gopaluni, R. (2000). An adaptive state-space based gpc with a two-degrees-of-freedom controller structure. In *IFAC Advanced Control of Chemical Processes*.
- Nakayama, T. and Washizu, K. (1981). The boundary element method applied to the analysis of two-dimensional nonlinear sloshing problems. *Int. J. for Numerical Methods in Engineering*, 17:1631–1646.
- Okatsuka, H., Matsuo, Y., and Inaba, T. (2002). Sloshing-less manipulation of liquid in open-type containers, (in japanese). *Trans. of Simulation Technology Conference*, pages 161–164.
- Oshima, M. (2000). Model predictive control (in japanese). *Trans. of the Society of Instrument and Control Engineers (SICE)*, 39(5):321–325.
- Romero, V. and Ingber, M. (1995). A numerical model for 2-d sloshing of pseudoviscous liquids in horizontally accelerated rectangular containers. *Boundary Elements XVII*, pages 567–583.
- Shibuya, R., Okatsuka, H., Noda, Y., and Terashima, K. (2011). Transferring and tilt motion control of the liquid container to suppress sloshing by using gpc. In *IEEE/SICE International Symposium*, pages 1055–1060.
- Yano, K., Oguro, N., and Terashima, K. (2001). Starting control with vibration damping by hybrid shaped approach considering time and frequency specifications, (in japanese). *Trans. of the Society of Instrument and Control Engineers (SICE)*, 37(5):403–410.
- Yano, K. and Terashima, K. (2001). Robust liquid container transfer control for complete sloshing suppression. *IEEE Trans. on Control Systems Technology*, 9(3):483–493.